BOLETIN DE LA SOCIEDAD ESPAÑOLA DE
Cerámica y Vidrio
www.elsevier.es/bsecv

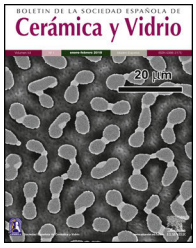

Ceramic foam decorated with ZnO for photodegradation of Rhodamine B dye

*Eduarda Medran Rangel**, *Caio César Nogueira de Melo*, *Fernando Machado Machado*

Technology Development Center, Federal University of Pelotas (UFPEL), Pelotas, RS, ZIP 96010-610, Brazil

ARTICLE INFO

Article history:
Received 5 April 2018
Accepted 17 October 2018
Available online 6 November 2018

Keywords:
Synthetic dye
Foam glass
Substrate
Porosity
Raw materials

ABSTRACT

The aim of this work was to prepare a foam glass (FG) decorated with nanostructured ZnO (FG/ZnO) and to evaluate its photocatalytic properties. The FG was sintered at 750 °C using fluorescent lamp glass residues and white eggshell as the foaming agent (FA). The ZnO nanostructured particles were deposited on FG via microwave-assisted hydrothermal synthesis. To confirm the impregnation of the ZnO nanostructured particles onto the foam glass, images were obtained by scanning electron microscopy (SEM). The photodegradation of Rhodamine B (RB) synthetic dye was investigated over the FG/ZnO, and an interesting degradation rate of RB dye was found. The results obtained were satisfactory and demonstrate that the use of foam glass as a support for ZnO is a viable alternative and of great interest for photocatalysis, especially since it requires further treatments for ZnO powder removal.

Espuma cerámica decorada con ZnO para la fotodegradación del colorante Rodamina B

Palabras clave:
Colorante sintético
Espuma vítrea
Substrato
Porosidad
Materia prima

RESUMEN

El objetivo de este trabajo fue preparar el vidrio espumado con nanoestructurados ZnO (FG/ZnO) y evaluar sus propiedades fotocatalíticas. El vidrio de espuma (FG) se sinterizó a 750° C y utilizando residuos de vidrio de lámpara de fluorescencia (FLGR) y cáscara de huevo blanco como agente espumante (FA). Las partículas nanoestructuradas de ZnO se depositaron en FG mediante síntesis hidrotermal asistida por microondas. Para confirmar la impregnación de las partículas nanoestructuradas de ZnO sobre el vidrio de espuma, las imágenes se obtuvieron por microscopía electrónica de barrido (SEM). La fotodegradación de Rodamina B (RB). el colorante sintético se investigó sobre el FG/ZnO, que mostró una interesante tasa de degradación del colorante RB. Los resultados obtenidos fueron satisfactorios y demuestran que el uso de polvo de ZnO es una alternativa viable y de gran interés para la fotocatálisis, especialmente porque requiere tratamientos adicionales de eliminación de polvo de ZnO.

* *Corresponding author.*
E-mail address: eduardamrangel@gmail.com (E.M. Rangel).
https://doi.org/10.1016/j.bsecv.2018.10.002

Introduction

Brazil has one of the largest economies of its continent and, with its population of 207.7 million inhabitants, generates more than 208,000 tonne of urban solid waste per day [1]. In the 1191 municipalities of the three southern states of the country, 22,322 tonnes of waste is generated per day. Of these, 70.7% is destined for landfills, 18.3% for controlled landfills, and 11% for waste disposal areas. In the state of Rio Grande do Sul, 8643 tonnes of waste is generated per day [2]. Among the residues generated are those coming from fluorescent lamps, which can result in contamination of the environment with mercury [3]. This metal can remain bioavailable for several years in several environmental compartments and can cause various types of damage to living things [4]. Around 100 million fluorescent lamps are consumed annually in Brazil and 94% are disposed of in landfills without due precautions [5]. In this sense, it is of great interest to develop new technologies and/or new materials using these residues as raw material and thus minimizing the environmental impacts.

Glass waste can be used as aggregates for Portland cement and asphalt concrete [6] as well as in the production of foam glass (FG) [7], a porous material used as a thermal and acoustic insulator with thin walls of individual cells filled with gas phase [8,9]. In this way, fluorescent lamp residues can be attractive in the manufacture of FG, providing an application for this type of residue and mitigating negative environmental impacts.

Wastewater generated by industry is also of great environmental concern. Among the various industrial segments, the textile sector stands out. In the environmental scenario, it presents itself as a potential polluter due to its characteristics that are highly harmful to the environment and it is one of the largest consumers of industrial water in the world [10]. Its average consumption is 100 L of water for 1 kg of textile material; thus with a total processed quantity of 30 million tonnes of textiles per year, the estimated total consumption is 3000 million cubic metres of water per year [11]. In addition to the large-scale use of water, another notable characteristic of the textile industry is the large amount of dyes used, resulting in the generation of effluents with a high level of colour [12]. Approximately 100,000 types of commercial dyes are known and used in various applications, comprising an annual production of 700,000 tonnes. Of this total production, approximately 10,000 tonnes are destined for consumption by the textile industry. About 100 tonnes of dye per year is inappropriately discarded in aquatic courses by the textile industry [13].

Among the different synthetic dyes, Rhodamine B (RB) stands out. This dye is recognized for its good stability and is widely used in the textile industry to dye silk, wool, leather, and cotton. Due to its widespread use, this dye is constantly found in water resources [14,15]. Some studies have reported that this organic compound may have carcinogenic and teratogenic effects on living organisms [16,17] when discarded incorrectly. The molecular structure of RB is presented in Fig. 1.

Several methods for the removal of dye from textile effluents have been suggested over time [17,18]. Photocatalysis, an advanced oxidation technique, is an attractive option for the treatment of textile effluents because it is an environmentally friendly method with in situ generation of hydroxyl radicals (OH), which are strongly oxidizing, and uses stable photocatalysts and non-toxic processes leading to complete degradation of contaminants from the textile industry [19–22]. This technique uses a photocatalyst that has the potential to transform recalcitrant organic contaminants into relatively harmless end products such as CO_2 and H_2O without generating secondary pollutants [23].

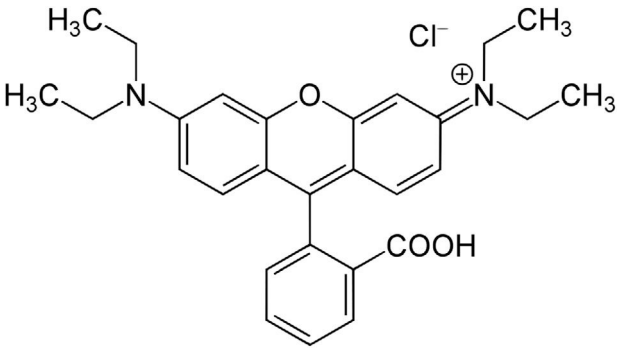

Fig. 1 – Molecular structure of RB dye.

One of the most important metal oxides with a range of applications is zinc oxide (ZnO). ZnO is a band gap semiconductor in the range of 3.2 eV and is widely used in dispersed form as a photocatalyst due to the low cost of obtaining it as well as its good catalytic properties [24]. However, use in the suspended form necessitates a separation step, which may be done through filtration processes [25], nanofiltration [26], microfiltration [27], or centrifugation [28]. It is worth mentioning that such processes are expensive and time consuming. In the last decades, the use of supports for the immobilization of photocatalysts has been gaining attention. Among the proposed supports are zeolites [29], polystyrene [30], silica [31], graphite carbon nitride [32], activated charcoal [33], and glass fibre [34].

The FGs are very attractive for application as photocatalyst supports, because their high porosity gives these materials a large contact area, allowing deposition of the substrate and thus increasing the photocatalytic effect. In this context, the objective of this work is to use FG produced by fluorescent lamp glass residues (FLGR) and eggshell as a substrate for the deposition of ZnO nanostructured particles and to evaluate the photodegradation efficiency of this system in the degradation of RB dye in aqueous solution.

Materials and methods

Material precursors and synthetic dye

Previously decontaminated FLGR, donated by Recilux (Canoas, RS, Brazil), and eggshell without the internal film, received from local businesses, were used for the production of FG. ZnO nanostructured particles were commercially available from Synth as the analytical standard.

The phase structure of the ZnO nanostructured particles was determined by X-ray diffraction (XRD, Bruker D2 PHASER

diffractometer) equipped with a Cu anode (CuKα radiation, λ = 1.5406 Å) operating at 30 kV and 10 mA. Measurements were carried out over the 2θ range of 10–80° with a scanning step width of 0.05° and time of 1 s. The crystallite size of the ZnO was determined by the X-ray line broadening method using the Scherer equation [35–37]. This measurement was carried out over the 2θ range of 33–39.5° with a scanning step width of 0.01° and time of 8 s. X-ray profile of standard highly crystalline silicon was used to make instrumental broadening corrections. The full-width at half maximum (FWHM) and constant of proportionality (Scherrer constant) $K = 0.9$ were used in the measurement [35–38].

The ZnO particles were also analyzed by scanning electron microscopy (SEM) in a JEOL microscope (model JSM-6610LV).

The optical characterization of ZnO nanostructured particles was performed by diffuse reflectance spectroscopy with the Kubelka-Munk remission function [35]. The optical band gap energy of the nanostructured ZnO was determined by Ocean Optics equipment (model DH-20000) equipped with an Ocean Optics integrating sphere (model ISP-REF). The band gap measurement of the semiconductors includes the excitation of electrons from the valance band to conduction band using photons of selected frequency [35].

The RB synthetic dye ($C_{28}H_{31}ClN_2O_3$, MW: 479.01 g mol^{-1}, CAS Number 81-88-9) was furnished by Synth (as analytical standard). The dye was used without further purification.

FG preparation

Fluorescent lamp glass and eggshell were ground separately in a ball mill and sieved in a 74 μm (#200, ABNT) sieve. Afterwards, the formulation was made for the production of FG with 7% foaming agent (FA) by mass [39]. Eggshell was used as FA due to its ease of production and low environmental impact [39]. The prepared blend was moulded in a uniaxial press (Ribeiro, RP0003) under a compaction pressure of 40 MPa. The green bodies were dried in an oven at 100 °C for 24 h and then sintered in an electric oven at 750 °C at a heating rate of 150 °C h^{-1} for 30 min [39]. The chemical compositions of FLGR and eggshell were determined by the X-ray fluorescence (XRF) technique using Shimadzu equipment (XRF 1800 model). The XRD technique was used to verify the crystal structure of eggshell and glass. A Bruker D2 PHASER X-ray diffractometer equipped with a copper anode operated at 30 kV and 10 mA was used. To evaluate the mass loss of the eggshell during heating, thermogravimetric analysis (TGA) was performed in a Harrop STA-726 thermobalance up to 1000° C at a heating rate of 10 °C min^{-1}.

Production of FG decorated with ZnO

For the deposition of the semiconductor onto FG, ZnO nanostructured particles were dispersed in deionized water at a concentration of 170 mg L^{-1}. Five FGs with an area of 3.8 cm^2 were used under magnetic stirring for 1 h while submerged in the ZnO solution. After the stirring was completed, the FGs were located in a polytetrafluoroethylene reactor, sealed, placed in a microwave oven (Electrolux, MEF41, Brazil), and then heated to 160 °C for 15 min at a pressure of 0.49 MPa [40]. The resulting material, FGs decorated with ZnO (FG/ZnO), was oven dried at 200 °C for 90 min. To confirm the decoration of the FGs with the ZnO nanostructured particles by microwave-assisted hydrothermal synthesis, images were obtained by a JEOL microscope (model JSM-6610LV).

Table 1 – Chemical composition of the precursors of the FGs.

FLGR		Eggshell	
Analyte	%	Analyte	%
Si	76.4	Ca	92.3
Ca	11.6	Mg	1.5
Na	2.5	S	1.0
Al	1.9	P	0.8
K	1.9	Sr	1.2
Pb	1.1	Na	0.8
Ba	1.0	Si	1.1
Mg	0.9	Cl	0.3
P	0.9	Fe	0.5
Fe	0.8	K	0.2
S	0.4	Al	0.2
Y	0.3		
Sr	0.2		
Zr	0.1		

Photodegradation tests

For the photodegradation tests, a 50 mg L^{-1} solution of RB dye at pH = 6 was produced. In addition, a photocatalytic reactor with a volumetric capacity of 200 mL, made of transparent glass, was externally coated with PVC walls and a 160 W (λ > 380 nm) mercury lamp was used as the source of light radiation. Three tests of the photodegradation of the RB in the solution were performed in triplicate, the first without the presence of any photocatalyst, the second using the ZnO in suspension (at a concentration of 170 mg L^{-1}), and the third using the previously prepared FG/ZnO. Two-millilitre aliquots of the RB dye solution were collected after 0, 5, 10, 20, 40, and 60 min of contact with the abovementioned systems and their concentrations were determined by spectrophotometry using a UV-vis spectrophotometer (Molecular Devices, SpectraMax 190) at the maximum wavelength of the RB dye absorbance (554 nm).

Results and discussion

The elementary chemical composition of the precursor materials used in the production of FGs is presented in Table 1. From this, it is possible to observe that the process used in the decontamination of FLGR was efficient, since there are no traces of Hg, and thus the residue can be used safely in the manufacture of ceramic bodies [41]. Further, it is possible to verify that its composition consists mainly of compounds based on silicon (Si), calcium (Ca), and sodium (Na), in addition to small concentrations of other trace elements that are present in the composition of the glass during its production.

Fig. 2 shows the X-ray diffractograms of eggshell and FLGR. By means of the eggshell diffractogram, it is possible to observe maximum diffraction peaks at approximately 23°, 29°, 36°, 39°, 43°, 47°, and 48°, which are characteristic

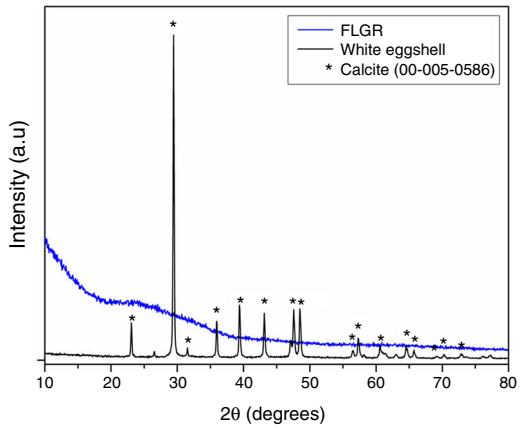

Fig. 2 – X-ray diffractograms of eggshell and FLGR.

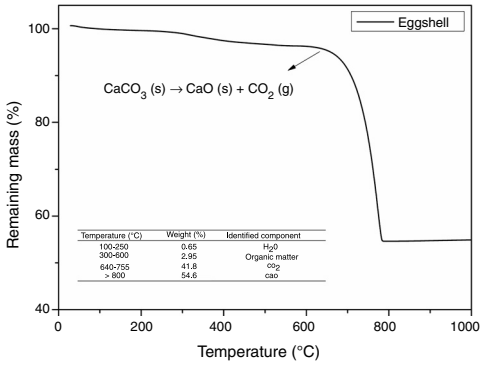

Fig. 3 – Thermogravimetric analysis of eggshell.

of calcium carbonate (calcite, $CaCO_3$, JPDS Card 00-005-0586), with a rhombohedral crystalline structure. This result is in agreement with the result obtained in the X-ray fluorescence analysis, which presents Ca as the predominant element in the composition of the eggshells. The X-ray diffractogram of the fluorescent lamp residue sample has a broad band between 20° and 40°, which is typical of an amorphous material [42].

Fig. 3 shows the thermogravimetric analysis of the eggshell sample. By means of this, the presence of three zones of mass loss can be observed: the first around 250 °C, attributed to the loss of the adsorbed water, the second at 300–600 °C, related to the decomposition of organic matter, and the third between 640 and 755 °C, attributed to the decomposition of $CaCO_3$. For eggshell, above 800 °C, predominantly CaO remains, as well as residues related to ash and inorganic compounds [43]. It is thus observed that eggshells at temperatures above 800 °C release part of their mass in the form of gases, particularly CO_2, which act as an FA in the molten glass. This indicates that the eggshell is a residue with potential application in the production of FGs.

Fig. 4 shows the X-ray diffractogram of ZnO nanostructured particles. It is possible to observe the presence of diffraction patterns characteristic of the zincite crystalline phase (JPDS Card 00-036-1451), which has a hexagonal crystalline system. Furthermore, through the Scherrer equation [35–38], it is possible to verify that the crystallite size of ZnO is approximately 75 nm. The crystallite size was estimated with the (101)

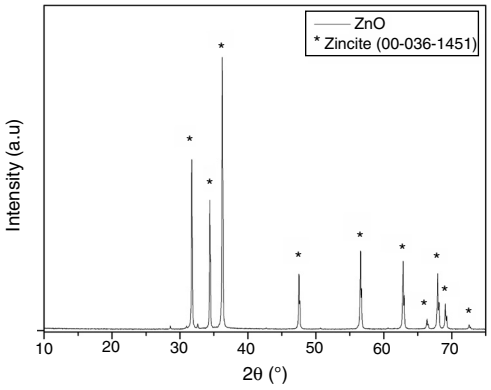

Fig. 4 – X-ray diffraction of ZnO nanostructured powder.

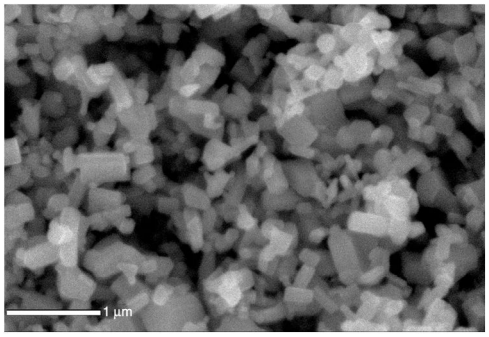

Fig. 5 – SEM of ZnO nanostructured particles.

diffraction peak (around 36.3°). This plane was chosen because it is the most prominent and well-marked [35–38].

The SEM image of the ZnO nanostructured particles (Fig. 5) shows the particles with a polyhedral shape, with dimensions greater than 100 nm.

Diffuse reflectance spectroscopy was utilized to determine the band gap of the ZnO nanostructured particles and to confirm the range of UV–vis radiation absorption of oxide. Fig. 6 shows the diffuse reflectance and Kubelka-Munk plot (in detail). It could be possible to check a similar performance of the absorbance–reflectance of the semiconductor oxides: the ZnO is transparent at 400–700 nm (visible region) [24,35]. In addition, at about 390 nm, a sharp increase in the absorbance is observed, which is attributed to the absorption edge. The

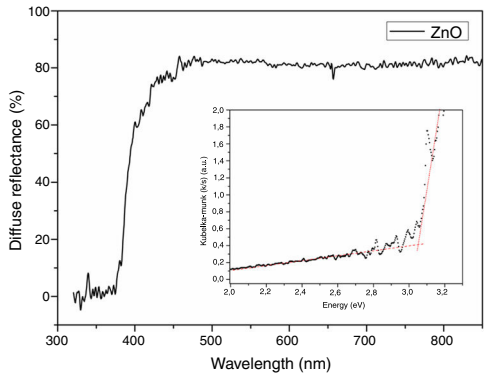

Fig. 6 – Diffuse reflectance of the ZnO nanostructured powder and Kubelka-Munk plot of the sample (in detail).

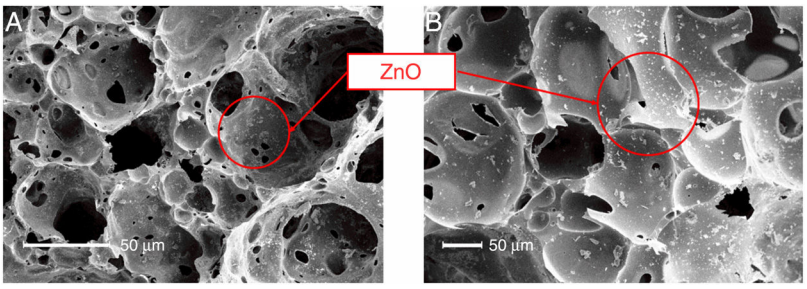

Fig. 7 – SEM of the (A) superficial view and (B) of the internal part of the FG/ZnO.

band gap energy of the oxide could also be obtained based on the onset of the Kubelka-Munk plot (shown in detail in Fig. 6) [35]. The optical band gap of ZnO particles calculated from the Kubelka-Munk remission function is 3.18 eV. This result agrees with those found in the literature [24,35].

SEM micrographs (Fig. 7) confirmed the presence of the ZnO powders on the surface (Fig. 7A) and inside (Fig. 7B) the FGs. As can be seen, the ZnO powders (white particles) decorated the entire porous surface of the sample (homogeneous recoating) and penetrated the internal pores of the FG structure. This result demonstrates that the methodology adopted here using microwaves as a decoration method was efficient for the production of the FG/ZnO system.

The results of photodegradation of the RB dye are shown in Fig. 8. This result shows that ZnO in suspension presented higher photocatalysis of RB dye, reaching a photodegradation rate of 39.9%, followed by the FG/ZnO system, which showed a degradation efficiency of RB dye of 27.6%. The lamp without the photocatalyst had a degradation efficiency of 9.2%. It is observed, therefore, that the suspended ZnO showed a degradation efficiency higher than that presented by the FG/ZnO system, as has already been reported in the literature [44]. However, for practical purposes, the use of particulate matter is problematic due to the additional step of filtration which must be added to the process, thus generating higher costs for its use. Thus, the FG/ZnO system is attractive because it presents similar photocatalytic activity for the studied system and also because it does not require an additional stage of filtration to remove the photocatalytic agent.

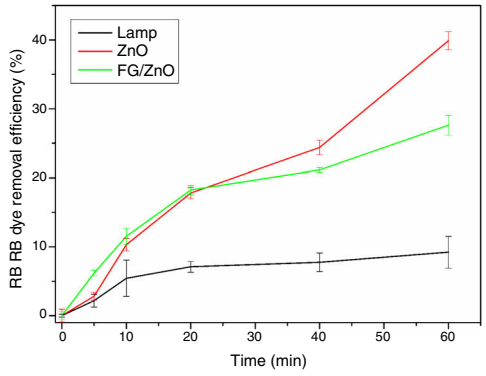

Fig. 8 – Photodegradation of RB tests with: solution only with the lamp, solution with ZnO in dispersion, and solution with the FG/ZnO. Conditions: 50 mg L^{-1} solution of RB dye at pH = 6.

Table 2 – Results of XRF for the FG/ZnO system before and after the photocatalysis.

Analyte	Before tests (%)	After tests (%)
Si	45.23	45.07
Ca	24.60	24.21
Zn	23.48	24.48
K	2.35	2.18
Ba	1.39	1.24
Pb	1.33	1.39
Fe	0.54	0.49
Sr	0.31	0.31
Y	0.22	0.24
Ac	0.17	0.13
Zr	0.12	0.15
Ir	0.10	–
Rb	0.05	0.05
Cu	0.05	–

In order to verify whether there was loss of ZnO to the solution after the photocatalytic tests, FG/ZnO samples were analyzed by XRF before and after the photocatalysis tests. Table 2 shows the presence of glass-forming elements [Si, Ca, and potassium (K), among others], Ca (present in eggshell), and zinc (from the decoration with ZnO). Other elements were detected in smaller quantities and are traces that are present in the composition of the glass during its production.

It is possible to observe that the percentage of Zn remained practically the same after the application of the FG decorated in the photocatalytic tests (variation within the error range of the detector of the equipment). This indicates that the decoration process was successfully performed and eliminates concern about possible contamination of ZnO in the aqueous medium after the application of FGs for the treatment of aqueous effluents. Thus, from this result, we can conclude that the FG/ZnO constitutes a single step in the photocatalysis process, requiring no further filtration, because the adhered ZnO remains in the FG structure after the treatment.

Conclusions

The results show that it was possible to produce FG decorated with ZnO nanostructured powder with photocatalytic properties using a microwave-assisted route. The micrographs obtained by SEM show that the decoration of ZnO powder under the support material was superficial and internal. The results obtained in degradation of the RB dye using FG/ZnO were satisfactory by the proximity to the results of

nanostructured ZnO suspension, since by making use of a support for the semiconductor it is possible to eliminate the filtration step in the process. It was also possible to conclude that the material adhered completely to the FG, thus avoiding the need for a second process to separate the ZnO from the solution. Making use of recyclable waste to manufacture the carrier and eliminating the filtration step in heterogeneous photoprocesses eliminates additional costs while minimizing the environmental impacts generated by the incorrect disposal of such wastes. This makes the application of FG/ZnO in dye treatment systems in solution very attractive.

Acknowledgments

The authors thank the Coordination of Improvement of Higher Level Personnel – CAPES for the financial support to this project, the Recilux Company for the donation of the glass residues used in this work and the Laboratory of Ceramic Materials – LACER of the Federal University of Rio Grande do Sul/RS – UFRGS for the support in the analysis. We are also grateful to Centro de Microscopia Eletrônica da Zona Sul (CEME SUL – FURG) for the use of the SEM microscope.

REFERENCES

[1] F.C. Luz, M.H. Rocha, E.E.S. Lora, O.J. Venturini, R.V. Andrade, M.M.V. Leme, O.A. Olmo, Techno-economic analysis of municipal solid waste gasification for electricity generation in Brazil, Energy Convers. Manage. 103 (2015) 321–337.
[2] K.R. Brina, T.S. Carvalho, P.G. Ardenghi, L.B. da Silva, Micronuclei and other nuclear anomalies in exfoliated buccal cells of urban solid waste collectors and recyclers in southern Brazil, Chemosphere 193 (2018) 1058–1062.
[3] L. Viererbl, M. Vinš, Z. Lahodová, A. Fuksa, J. Kučera, M. Koleška, A. Voljanskij, Mercury mass measurement in fluorescent lamps via neutron activation analysis, Radiat. Phys. Chem. 116 (2015) 56–59.
[4] Q. Tan, J. Li, A study of waste fluorescent lamp generation in mainland China, J. Clean. Prod. 81 (2014) 227–233.
[5] M.M. Laruccia, J.V. Nascimento, G.J. Deghi, M.G. Garcia, A study of consumer behavior on recycling of fluorescent lamps in São Paulo, Brazil, Int. J. Bus. Admin. 2 (2011) 101–112.
[6] A. Pokorny, J. Vicenzi, C.P. Bergmann, Influence of the addition of alumina on the microstructure of the glass foam, Cerâmica 54 (2008) 97–102.
[7] N.M.P. Low, Formation of cellular-structure glass with carbonate compounds and natural mica powders, J. Mater. Sci. 16 (1981) 800–808.
[8] A. Pokorny, J. Vicenzi, C.P. Bergmann, Influence of heating rate on the microstructure of glass foams, Waste Manage. Res. 29 (2011) 172–179.
[9] H. Wang, K. Feng, Y. Zhou, Q. Sun, H. Shi, Effects of $Na_2B_4O_7\,5H_2O$ on the properties of foam glass from waste glass and titania-bearing blast furnace slag, Mater. Lett. 132 (2014) 176–178.
[10] E. Hu, S. Shang, X.M. Tao, S. Jiang, K.L. Chiu, Regeneration and reuse of highly polluting textile dyeing effluents through catalytic ozonation with carbon aerogel catalysts, J. Clean. Prod. 137 (2016) 1055–1065.
[11] A.T. Turcanu, T. Bechtold, Cathodic decolourisation of reactive dyes in model effluents released from textile dyeing, J. Clean. Prod. 142 (2017) 1397–1405.
[12] N.K.B. Kılıç, J.L. Nielsen, M. Yuce, G. Donmez, Characterization of a simple bacterial consortium for effective treatment of wastewaters with reactive dyes and Cr(VI), Chemosphere 67 (2007) 826–831.
[13] F.M. Machado, C.P. Bergmann, E.C. Lima, M.A. Adebayo, S.B. Fagan, Adsorption of a textile dye from aqueous solutions by carbon nanotubes, Mater. Res. 17 (2014) 153–160.
[14] J.O. Carneiro, A.P. Samantilleke, P. Parpot, F. Fernandes, M. Pastor, A. Correia, E.A. Luís, A.A. Chivanga Barros, V. Teixeira, Visible light induced enhanced photocatalytic degradation of industrial effluents (Rhodamine B) in aqueous media using TiO_2 nanoparticles, J. Nanomater. 2016 (2016) 1–13.
[15] S. Dhanavel, E.A.K. Nivethaa, K. Dhanapal, V.K. Gupta, V. Narayanand, A. Stephen, α-MoO_3/polyaniline composite for effective scavenging of Rhodamine B, Congo red and textile dye effluent, RSC Adv. 6 (2016) 28871–28886.
[16] E. Baldev, D. Mubarak Ali, A. Ilavarasi, D. Pandiaraj, K.A. Sheik Syed Ishackc, N. Thajuddin, Degradation of synthetic dye, Rhodamine B to environmentally non-toxic products using microalgae, Colloid Surf. B 105 (2013) 207–214.
[17] D.C. dos Santos, M.A. Adebayo, E.C. Lima, S.F.P. Pereira, R. Cataluña, C. Saucier, P.S. Thue, F.M. Machado, Application of carbon composite adsorbents prepared from coffee waste and clay for the removal of reactive dyes from aqueous solution, J. Braz. Chem. Soc. 26 (2015) 924–938.
[18] C.R. Holkar, A.J. Jadhav, D.V. Pinjari, N.M. Mahamuni, A.B. Pandit, A critical review on textile wastewater treatments: possible approaches, J. Environ. Manage. 182 (2016) 351–366.
[19] Q.I. Rahman, M. Ahmad, S.K. Misra, M. Lohani, Effective photocatalytic degradation of rhodamine B dye by ZnO nanoparticles, Mater. Lett. 91 (2013) 170–174.
[20] N. Jallouli, K. Elghniji, H. Trabelsi, M. Ksibi, Photocatalytic degradation of paracetamol on TiO_2 nanoparticles and TiO_2/cellulosic fiber under UV and sunlight irradiation, Arab. J. Chem. 10 (2017) 3640–3645.
[21] G. Zhang, G. Kim, Choi, Visible light driven photocatalysis mediated via ligand-to-metal charge transfer (LMCT): an alternative approach to solar activation of titania, Energy Environ. Sci. 7 (2014) 954–966.
[22] X.T. Hu, W. Mohamood, Ma, C. Chen, J. Zhao, Oxidative decomposition of Rhodamine B dye in the presence of VO^{2+} and/or Pt(IV) under visible light irradiation: n-deethylation, chromophore cleavage, and mineralization, J. Phys. Chem. B 110 (2006) 26012–26018.
[23] D. Maruthamani, D. Divakar, M. Kumaravel, Enhanced photocatalytic activity of TiO_2 by reduced graphene oxide in mineralization of Rhodamine B dye, J. Ind. Eng. Chem. 30 (2015) 33–43.
[24] M.T. Man, J.H. Kim, M.S. Jeong, A.T.T. Do, H.S. Lee, Oriented ZnO nanostructures and their application in photocatalysis, J. Lumin. 185 (2017) 17–22.
[25] S. Khaoulani, H. Chaker, C. Cadet, E. Bychkov, L. Cherif, A. Bengueddach, S. Fourmentin, Wastewater treatment by cyclodextrin polymers and noble metal/mesoporous TiO_2 photocatalysts, C.R. Chim. 18 (2015) 23–31.
[26] M. Mondal, S. De, Treatment of textile plant effluent by hollow fiber nanofiltration membrane and multi-component steady state modeling, Chem. Eng. J. 285 (2016) 304–318.
[27] W. Xi, S.U. Geissen, Separation of titanium dioxide from photocatalytically treated water by cross-flow microfiltration, Water Res. 35 (2001) 1256–1262.
[28] S. Buddee, S. Wongnawa, U. Sirimahachai, W. Puetpaibool, Recyclable UV and visible light photocatalytically active

amorphous TiO_2 doped with M (III) ions (M = Cr and Fe), Mater. Chem. Phys. 126 (2011) 167–177.
[29] M. Karimi-Shamsabadi, A. Nezamzadeh-Ejhieh, Comparative study on the increased photoactivity of coupled and supported manganese-silver oxides onto a natural zeolite nano-particles, J. Mol. Catal. A Chem. 418–419 (2016) 103–114.
[30] R. Ata, O. Sacco, V. Vaiano, L. Rizzo, G.Y. Tore, D. Sannino, Visible light active N-doped TiO_2 immobilized on polystyrene as efficient system for wastewater treatment, J. Photochem. Photobiol. A 348 (2017) 255–262.
[31] Z.Y. Shen, L.Y. Li, Y. Li, C.C. Wang, Fabrication of hydroxyl group modified monodispersed hybrid silica particles and the h-SiO2/TiO_2 core/shell microspheres as high performance photocatalyst for dye degradation, J. Colloid Interf. Sci. 354 (2011) 196–201.
[32] Y. Zheng, Z. Zhang, C. Li, Beta-FeOOH-supported graphitic carbon nitride as an efficient visible light photocatalyst, J. Mol. Catal. A: Chem. 423 (2016) 463–471.
[33] P. Muthirulan, M. Meenakshisundararam, N. Kannan, Beneficial role of ZnO photocatalyst supported with porous activated carbon for the mineralization of alizarin cyanin green dye in aqueous solution, J. Adv. Res. 4 (2013) 479–484.
[34] T.D. Pham, B.K. Lee, Disinfection of *Staphylococcus aureus* in indoor aerosols using Cu-TiO_2 deposited on glass fiber under visible light irradiation, J. Photochem. Photobiol. A 307–308 (2015) 16–22.
[35] R. Camaratta, J.O. Messana, C.P. Bergmann, Synthesis of ZnO through biomimetization of eggshell membranes using different precursors and its characterization, Ceram. Int. 41 (2015) 14826–14833.
[36] H. Sarma, K.C. Sarma, X-ray peak broadening analysis of ZnO nanoparticles derived by precipitation method, Int. J. Sci. Res. Public (IJSRP) 4 (2014) 1–7.
[37] S.K. Esthappan, A.B. Nair, R. Joseph, Effect of crystallite size of zinc oxide on the mechanical, thermal and flow properties of polypropylene/zinc oxide nanocomposites, Compos. Pt. B: Eng. 69 (2015) 145–153.
[38] Y. Köseoğlua, A simple microwave-assisted combustion synthesis and structural, optical and magnetic characterization of ZnO nanoplatelets, Ceram. Int. 40 (2014) 4673–4679.
[39] E.M. Rangel, C.C.N. de Melo, C.O. Carvalho, A.G. Osorio, F.M. Machado, Synthesis and characterization of foam glass from solid waste, Rev. Mater. 23 (2018) 1–10.
[40] W.M. Ventura, D.C. Batalha, H.V. Fajardo, J.G. Taylor, N.H. Marins, B.S. Noremberg, T. Tański, N.L.V. Carreño, Low temperature liquid phase catalytic oxidation of aniline promoted byniobium pentoxide micro and nanoparticles, Catal. Commun. 99 (2017) 135–140.
[41] C.M.F. Vieira, A.S.C. Morais, S.N. Monteiro, G.C.G. Delaqua, Industrial test of heavy clay ceramic incorporated with fluorescent lamp waste, Ceramic 62 (2016) 376–385.
[42] C. Mugoni, M. Montorsi, C. Siligardi, F. Andreola, I. Lancellotti, E. Bernardo, L. Barbieri, Design of glass foams with low environmental impact, Ceram. Int. 41 (2015) 3400–3408.
[43] E. Mosaddegh, A. Hassankhani, Preparation and characterization of nano-CaO based on eggshell waste: novel and green catalytic approach to highly efficient synthesis of pyrano[4,3-b]pyrans, J. Catal. 35 (2014) 351–356.
[44] E.M. Rangel, C.O. Carvalho, D.R. Arsand, Synthesis of foam glass with immobilized zinc oxide for photodegradation of Alizarin S in aqueous solution, S. Braz. J. Chem. 29 (2018) 75–79.